# Photochemically Driven Nickel-Catalyzed Carboxylative C-N Coupling: Scope and Mechanism

Seifallah Abid,<sup>[a, +]</sup> Kevin P. Quirion, <sup>[b, +]</sup> Yi Yang, <sup>[a, +]</sup> Renhe Tang,<sup>[a]</sup> Binh Khanh Mai, <sup>[b]</sup> Peng Liu,\*<sup>[b]</sup> and Anis Tlili\*<sup>[a]</sup>

- [a] Dr. S. Abid, Y. Yang, R. Tang, Dr A. Tlili
   Univ Lyon, CNRS, Université Claude Bernard Lyon 1, ICBMS, UMR5246
   43 Bd du 11 Novembre 1918, 69622 Villeurbanne, France
   E-mail: anis.tlili@univ-lyon1.fr
- K. P. Quirion, B. K. Mai, Prof. P. Liu
   Department of Chemistry, University of Pittsburgh
   Pittsburgh, Pennsylvania 15260(USA)

   E-mail: <a href="mailto:pengliu@pitt.edu">pengliu@pitt.edu</a>
- [+] These authors contributed equally

Supporting information for this article is given via a link at the end of the document.((Please delete this text if not appropriate))

**Abstract:** Herein we disclosed an unprecedented photochemically driven nickel-catalyzed carboxylative Buchwald-Hartwig amination to access a wide range of aryl carbamate derivatives. This reaction is performed under mild condition of temperature and atmospheric pressure of CO<sub>2</sub> starting from commercially available (hetero)aryl iodides/bromides derivatives and alkyl amines preventing the formation of hazardous and/or toxic waste. Moreover, preliminary mechanistic investigation including stochiometric experiments as well as DFT calculations allows us to shed the light on the reaction mechanism.

#### Introduction

Transition-metal (TM) catalyzed cross-coupling reactions between aryl (pseudo)halides and carbon or heteroatom nucleophiles have revolutionized the way new bonds are assembled.[1] The robustness of this technology to forge C-C and C-heteroatom bonds is routinely demonstrated in academia and in large scale industrial applications. [1, 2] In addition to classical cross-coupling reactions, three-component transition metalcatalyzed carbonylative methodologies using carbon monoxide are another efficient approach to construct complex molecules.[3] For such processes, the key to success is the insertion of carbon monoxide into the metal-aryl bond due to its high reactivity. For example, direct access to valuable amides could be achieved through the cross-coupling of aryl halides and amines in the presence of carbon monoxide under transition metal catalysis (Scheme 1).[4] On the other hand, carbon dioxide is the most important greenhouse gas on Earth. Its concentration has exceeded the 400-ppm level in the atmosphere and to date only few industrial processes enable CO2-based transformations due to its thermodynamic and kinetic stability. [5] Complementary to the chemistry of carbon monoxide, the design of three-component reactions making use of CO2 will allow the formation of highly complex scaffolds. As an example, aryl carbamate derivatives are valuable compounds that are usually obtained from hazardous chemicals while generating highly toxic waste. [6] A threecomponent reaction with carbon dioxide would offer a more effective route to access aryl carbamates (Scheme 1).

TM catalyzed Buchwald-Hartwig amination

TM catalyzed carbonylative Buchwald-Hartwig amination

**This work**: Dual Nickel/Photocatalysis catalyzed carboxylative Buchwald-Hartwig amination

$$X + HNR^{1}R^{2} \frac{[Ni]/PC}{CO_{2}}$$
visible-light

**Scheme 1.** State of the art on the Buchwald-Hartwig amination, carbonylative amination and introduction of the new concept.

Surprisingly, while from a simple retrosynthetic analysis, the reductive elimination from [TM](OC(O)NR<sup>1</sup>R<sup>2</sup>)Ar may lead to the formation of the desired aryl carbamate (ArOC(O)NR<sup>1</sup>R<sup>2</sup>) product, to date, no example of metal-catalyzed carboxylative cross-coupling of aryl halides with amines have been reported. This is certainly due to two mechanistic questions that have to be considered:  $\it i$ ) Although amine reacts with atmospheric pressure of CO<sub>2</sub> to generate carbamate,<sup>[7]</sup> the reactivity of such species with transition metal has not been reported yet;  $\it ii$ ) The C-O reductive elimination of [TM](OC(O)NR<sup>1</sup>R<sup>2</sup>)Ar to forge C(sp<sup>2</sup>)-OC(O)NR<sup>1</sup>R<sup>2</sup> is also an unknown fundamental step.

DPA

Unlocking these critical steps of the catalytic cycle will pave the way to the development of a robust carboxylative process to easily access aryl carbamate derivatives. Recent results by the Macmillan group demonstrated that the reductive elimination of [Ni](OC(O)R)Ar for the synthesis of esters could take place under energy transfer (EnT) catalysis with an [Ir] photocatalyst.[8] In addition, a similar strategy was developed by the groups of Li, Huang and Zhang where the authors successfully replaced the [Ir] catalyst with a cyanoarene organophotocatalyst. [9] These examples highlight that a combination of a photocatalyst with transition metal catalysis can promote challenging reductive elimination.[10] Based on this principle, we report herein a photochemically driven nickel-catalyzed carboxylative Buchwald-Hartwig amination to access a wide range of aryl carbamate derivatives. It should be mentioned that a related work developed by Repo group appeared recently[11]

## **Results and Discussion**

To confirm the feasibility of this concept we selected p-iodobenzotrifluoride as model substrate with diethyl amine as coupling partner under atmospheric pressure of  $CO_2$  and white light irradiation (2\*27 W CFL). To our delight 80% of the desired product was obtained by using 5 mol% of air stable NiBr<sub>2</sub>.diglyme in conjunction with 5 mol% 4,4'-dtbbpy as ligand and  $Cs_2CO_3$  as base using **PC1** (5CzBN, 1 mol%) as photocatalyst. Herein, the choice of this photocatalyst was guided by the triplet energy ( $E_T$ , 2.68 eV)<sup>[9]</sup> higher than that of  $Ir(ppy)_3$  (2.33 eV) used in the Macmillan system.<sup>[8a]</sup>

Table 1. Optimization of nickel/ligand precursors.

$$F_{3}C \xrightarrow{F_{3}C} + CO_{2} + Et_{2}NH \xrightarrow{S \text{ mol% NiBr}_{2} \text{ diglyme}} + CO_{2} + Et_{2}NH \xrightarrow{S \text{ mol% L3}} + CO_{2} + Et_{2}NH \xrightarrow{C_{3}CO_{3} (2 \text{ equiv.})} + CO_{2} + Et_{2}NH \xrightarrow{C_{3}CO_{3} (2 \text{ equiv.})} + CO_{2} + CO_{2} + CO_{2} + CO_{3} + CO_{3}$$

1 mol% PC1

Entry <sup>[a]</sup>	Deviation from Standard conditions	Yield [%] <sup>[b]</sup>
1	None	80
2	NiBr <sub>2</sub> .DME instead of NiBr <sub>2</sub> .diglyme	77
3	NiCl <sub>2</sub> .DME instead of NiBr <sub>2</sub> .diglyme	52
4	Ni(acac) <sub>2</sub> instead of NiBr <sub>2</sub> .diglyme	34
5	Ni(COD) <sub>2</sub> instead of NiBr <sub>2</sub> .diglyme	80
6	L1 instead of L3	60
7	L2 instead of L3	76
8	L4 instead of L3	29

[a] Reactions were performed with 1a (0.2 mmol, 1 equiv), HNEt $_2$  (0.4 mmol, 2 equiv), CO $_2$  (1 atm), PC1 (1 mol%), NiBr $_2$ .diglyme (5 mol%), L3 (5 mol%), Cs $_2$ CO $_3$  (0.4 mmol, 2 equiv) and DMF (2 mL). The reaction mixture was stirred at RT for 16 hours under 2\*27W CFL unless otherwise noted [b] Determined by  $^{19}$ F NMR spectroscopy with PhOCF $_3$  as an internal standard.

With this proof of concept in hand, initial focus was devoted to the optimization of the nickel/ligand catalytic system. NiBr<sub>2</sub>.DME shows higher reactivity in comparison to NiCl<sub>2</sub>.DME (Table 1, entries 2&4). Ni(acac)<sub>2</sub> was also effective under our reaction conditions albeit in low yield of 34% (Table 1, entries 4). The use of air sensitive Ni(COD)<sub>2</sub> allow the formation of the desired product in an excellent yield of 80% (Table 1, entries 5). Afterwards, bipyridine type ligands were investigated. While simple bipyridine afforded lower reactivity of 60%, the use of electron rich 4,4-diMeObpy furnished the desired product in 76% yield. The presence of di-Me group in 6,6' position is detrimental to the reaction since only 29% of the desired product was observed (Table1, entry 8).

Table 2. Reaction optimization

$$F_{3}C \begin{tabular}{lll} & & & & & & & & \\ & & & & & & & \\ & & & & & & \\ & & & & & \\ & & & & & \\ & & & & \\ & & & & \\ & & & & \\ & & & \\ & & & \\ & & & \\ & & & \\ & & & \\ & & & \\ & & & \\ & & \\ & & & \\ &$$

Entry <sup>[a]</sup>	Deviation from Standard conditions	Yield [%] <sup>[b]</sup>
1	None	80
2	K <sub>2</sub> CO <sub>3</sub> instead of Cs <sub>2</sub> CO <sub>3</sub>	65
3	K <sub>3</sub> PO <sub>4</sub> instead of Cs <sub>2</sub> CO <sub>3</sub>	48
4	CsF instead of Cs <sub>2</sub> CO <sub>3</sub>	71
5	NEt <sub>3</sub> instead of instead of Cs <sub>2</sub> CO <sub>3</sub>	15
6	DBU instead of instead of Cs <sub>2</sub> CO <sub>3</sub>	60
7	DMA instead of DMF	76
8	DMSO instead of DMF	23
9	MeCN instead of DMF	2
10	PC2 instead of PC1	61
11	PC3 instead of PC1	52
12	PC4 instead of PC1	74
13	Ir(ppy)₃ instead of PC1	70
14	Ir[dF(tbu)-ppy]₃ instead of PC1	65
15	No light	0
16	No PC1	0
17	0.1 mol% of PC1 instead of 1 mol%	85 (83%) <sup>[c]</sup>
18	pCF <sub>3</sub> PhBr instead of pCF <sub>3</sub> PhI	74 (69%) <sup>[c]</sup>

[a] Reactions were performed with 1a (0.2 mmol, 1 equiv), HNEt<sub>2</sub> (0.4 mmol, 2 equiv), CO<sub>2</sub> (1 atm), PC1 (1 mol%), NiBr<sub>2</sub>.diglyme (5 mol%), L3 (5 mol%), Cs<sub>2</sub>CO<sub>3</sub> (0.4 mmol, 2 equiv) and DMF (2 mL). The reaction mixture was stirred at RT for 16 hours under 2\*27W CFL unless otherwise noted [b] Determined by  $^{19}\text{F}$  NMR spectroscopy with PhOCF<sub>3</sub> as an internal standard. [c] Isolated Yield.

Then, we investigated other reaction parameters (Table 2). First, the impact of several bases on the reaction outcome was assessed. To some extent, K<sub>2</sub>CO<sub>3</sub> showed interesting reactivity and 65% yield of **2a** was obtained. Lower product formation was observed with K<sub>3</sub>PO<sub>4</sub> (table 2, entry 3). Interestingly, the use of CsF provided good reactivity and the desired product **2a** was obtained in 71% yield (table 2, entry 4). The use of organic bases was also investigated. While NEt<sub>3</sub> furnishes the desired product in only very low yield of 15%, DBU showed good compatibility and 60% of **2a** was obtained (table 2, entries 15&16). Regarding the solvent, similar reactivity was observed in DMA but very low amount or traces of product were observed in DMSO and MeCN, respectively (Table 1, entries 7-9). Several photocatalysts were

also investigated. Cyanoarenes **PC2-PC4** were effective and yields up to 74% were obtained (table 1, entries 10-14). Similarly, [Ir] based photocatalyst showed interesting reactivity although with lower efficiency than **PC1** (Table 1, entries 13&14). Control experiments without light or without **PC1** demonstrated the importance of both the light and the presence of the organophotocatalyst since no product formation was observed (table 2, entries 15&16). To our delight, decreasing the

organophotocatalyst loading to 0.1 mol% afforded product **2a** in 85% yield (Table 1, entry 17). Finally, the use of *p*-bromobenzotrifluoride was also effective under our reaction conditions and the corresponding product **2a** was obtained in very good yield of 74% (Table 2, entry18).

Scheme 2. Substrate scope: [a] Reactions were performed with 1 (0.2 mmol, 1 equiv.), amine (0.4 mmol, 2 equiv.), CO<sub>2</sub> (1 atm), PC1 (0.1 mol%), NiBr<sub>2</sub>.diglyme (5 mol%), L3 (5 mol%), Cs<sub>2</sub>CO<sub>3</sub> (0.4 mmol, 2 equiv) and DMF (2 mL). The reaction mixture was stirred at RT for 16 hours unless otherwise noted. Yield of isolated products. [b] Determined by <sup>19</sup>F NMR spectroscopy with PhOCF<sub>3</sub> as an internal standard. [c] Determined by <sup>1</sup>H NMR spectroscopy with 1,3,5-trimehtoxybenzene as an internal standard.

With the optimized set of conditions in hand, we turned our attention to studying the scope of the carboxylative Buchwald-Hartwig amination. The use of several (hetero)aryl iodides and bromides was first investigated. Trifluoromethyl substituted iodoas well as bromoarene were converted with low to very good yield (products 2a-c up to 77%). Arenes substituted with cyano groups were successfully employed under the reaction conditions and the desired products were obtained in excellent yields up to 87% (products 2d & 2e). The presence of ester groups either in the para or meta position was also tolerated under our protocol and the corresponding products were obtained in excellent yields either by starting from the iodo- or bromoaryl derivatives (products 2f & 2g). Moreover, the use of sensitive functional groups toward basic conditions including acetyl and aldehyde were successfully converted to the desired product with moderate to very good yields (products 2f & 2i). Simple naphthalene and biphenyl starting material were smoothly converted to the desired carbamate derivatives with yields up to 82% (products 2i & 2j). Afterwards, pharmaceutically relevant heterocyclic pyridinebased iodo and bromo derivatives were subjected to our protocol. The presence of methyl as an electron donating group allows the formation of the desired product in synthetically useful yield of 53% (product 21). lodo- and bromopyridines substituted with CF<sub>3</sub> group are also tolerated under this protocol and the desired trifluoromethylpyridine carbamate were obtained in excellent yields up to 90% (products 2m-2o). Finally, the use of iodoaryl substituted either with boronic acid pinacol ester or bromo groups were converted to the desired corresponding aryl carbamate with yields up to 80% (products 2p-2q). Herein, post functionalization under cross-coupling reaction conditions is envisioned as a follow-up reaction. After observing good reactivity with different aryl iodides and bromide, we decided to investigate the scope of different amines derivatives. Other dialkylamine derivatives also showed excellent compatibility with our protocol including bulky di-iPr- and di-tBu-amines and the corresponding aryl carbamate were obtained in very good yields up to 75% (product 2fa and 2fb). Benzyilic amines were also tolerated under our reaction conditions and the desired aryl carbamates were obtained in excellent yields (2fc, 2fd and 2fe). The use of cyclic amine was also successfully investigated. Indeed, piperidine and morpholine turned out to be good amines coupling partners under our protocol (product 2ff and 2fg). Similarly, piperazine derivatives turned out to be effective for the synthesis of aryl carbamates (product 2fh and 2fi). Moreover, an excellent yield of 90% for aryl carbamate 2fm was achieved starting from pyrrolidine as amine coupling partner. Finally, the use of pharmaceutically relevant amines was also investigated. Desipramine, Nortriptyline as well as Maprotiline were successfully coupled for the synthesis of aryl carbamates and the corresponding desired products were obtained in excellent yields up to 91% (products 2fk, 2fl and 2fm).

After observing general reactivity with (hetero)aryl iodide and bromide as well as different amines coupling partners, we turned our attention to the investigation of the reaction mechanism by performing several control experiments. As observed in the optimization of the reaction,  $Ni(COD)_2$  is an active precatalyst for the carboxylative Buchwald-Hartwig amination (Table 1, entry 5). Herein, we envisioned that the oxidative addition of the aryl halide is a plausible first step for the catalytic cycle. In this context, we synthesized the **Ni-I** complex resulting from the oxidative addition of the *t*Bubpy nickel(0) complex and the 4-bromobenzotrifluoride. This complex was then stoichiometrically submitted to the

reaction conditions in the presence of 1 mol% of PC1. Surprisingly, no desired product was observed. Instead, 60% of the reduced product PhCF<sub>3</sub> was detected in <sup>19</sup>F NMR (Scheme 3, entry 1). Herein, the photochemical homolysis of the Ni-C<sub>6</sub>H<sub>4</sub>CF<sub>3</sub> bond could occur as already reported by Doyle[12] and Hadt[13] followed by HAT to form the reduced PhCF<sub>3</sub>. Although this Ni(II) complex is not effective for the synthesis of aryl carbamate under stochiometric conditions, it turned out to be catalytically active for the formation of the desired product 2a in 80% yield by <sup>19</sup>F NMR (Scheme 3, entry 2). The photodegradation of complex Ni-I was confirmed in the presence of 1 mol% of PC1 under irradiation to give PhCF<sub>3</sub>. (Scheme 3, entry 3). As previously reported, the photolysis of the Ni(II)-PhCF3 bond is expected to lead to a Ni(I) species that may be active for the desired cross-coupling reaction. Indeed, when the photolysis reaction is carried out in the presence of an external aryl iodide 1f in the reduced PhCF3 is formed along with the formation of compound 2f in 99% yield indicating the formation of an active nickel precatalyst in situ (Scheme 3, entry 4).

Scheme 3. Preliminary mechanistic investigations

In order to get more insights into the reaction mechanism, we performed density functional theory (DFT) calculations to investigate the Ni(4,4'-dtbbpy)-catalyzed carboxylative amination of aryl iodide 1a with dimethyl amine as the model substrate. [14] We first examined the Ni(0)-Ni(II) pathway[8] that initiates from a nickel(0) active catalyst  $^{1}6$  (Figure 1). A three-centered oxidative addition ( $^{1}TS1$ ) of aryl iodide 1a forms an arylnickel(II) iodide ( $^{1}7$ ), which then proceeds through ligand exchange with cesium carbamate 4 to form  $^{1}9$ . The formation of cesium carbamate[15] 4 from CO<sub>2</sub>, amine, and Cs<sub>2</sub>CO<sub>3\*</sub>(DMF)<sub>2</sub> ( $\Delta G = -17.8$  kcal/mol, Figure 1a), the aryl iodide oxidative addition ( $\Delta G = -46.1$  kcal/mol), and the ligand exchange with cesium carbamate ( $\Delta G = -15.1$  kcal/mol) are all exergonic, the resulting nickel(II) carbamate  $^{1}9$  is highly thermodynamically stable. The direct C–O reductive

elimination (RE) from 19 requires an insurmountable barrier of 43.4 kcal/mol (TS2) and is endergonic by 29.4 kcal/mol. This is consistent with previous computational studies that indicate the Ni(II)-Ni(0) C-O reductive elimination is challenging<sup>[16]</sup> whereas the reverse reaction—Ni(0)-Ni(II) oxidative addition of aryl carbamates—was exergonic by more than 25 kcal/mol.[17] Based on previous computational studies by Chen<sup>[16a]</sup> and Guan<sup>[16b]</sup> and experimental studies by MacMillan and Scholes [8b] that suggested the C-O(carboxylate) RE of Ni(II)(aryl) acetate complexes can be promoted by an energy transfer (EnT) process with iridium photocatalysts, we performed TD-DFT calculations to study the excitation-promoted C-O RE pathway to form aryl carbamate. Our calculations indicated that the adiabatic excitation of arylnickel(II) carbamate 19 leads to a metal-to-ligand charge transfer (MLCT) complex 39(MLCT) [18] with an adiabatic excitation energy of 34.0 kcal/mol. This MLCT complex involves singleelectron excitation from a metal d orbital to the  $\pi^*$  orbital on the ligand (see Figure S1), thus leading to nickel(III) character that promotes C-O RE. The computed barrier for C-O RE from the MLCT complex <sup>3</sup>9<sup>(MLCT)</sup> is 24.8 kcal/mol, which is substantially lower than the C-O RE from ground state nickel(II) 19. The MLCT C-O RE transition state (3TS2(MLCT)) and the corresponding singlet 1TS2 are both square planar, although the former has a significantly longer forming C-O bond (1.97 Å compared to 1.72 Å in <sup>1</sup>TS2), indicating an earlier TS consistent with the Hammond postulate.

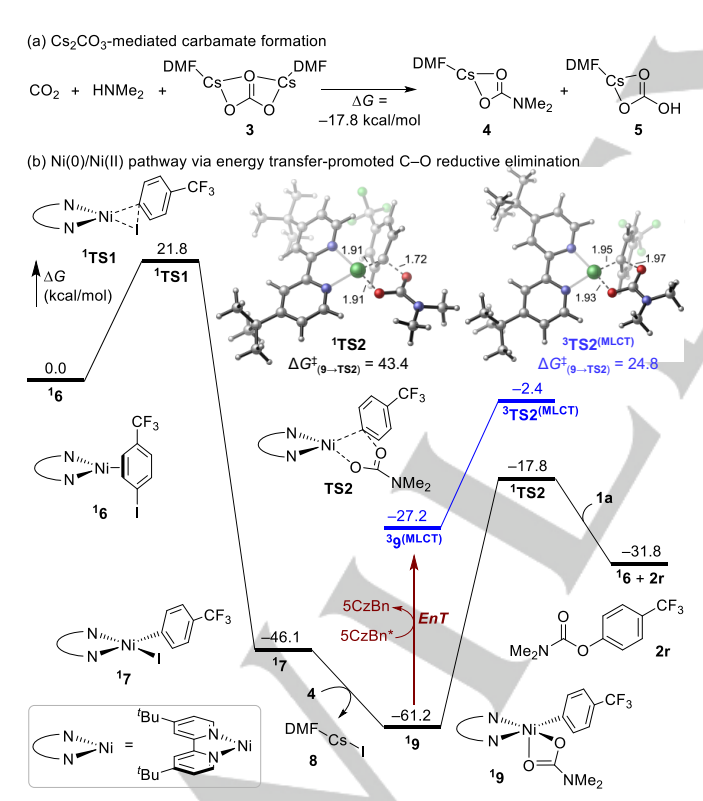


Figure 1. Computed reaction energy profile of the Ni(0)/Ni(II) pathway. 14

Next, we considered an alternative mechanism with nickel(I) iodide <sup>2</sup>10 as the active catalyst (Figure 2). The nickel(I) species may be formed via either SET from the photocatalyst to NiBr<sub>2</sub> precatalyst,<sup>[19]</sup> or photochemical homolysis of arylnickel(II) halide<sup>[12, 13, 20]</sup> (see Scheme 3). Because the ligand exchange to afford nickel(I) carbamate <sup>2</sup>11 is exergonic by 10.6 kcal/mol, the aryliodide oxidative addition (<sup>2</sup>TS3) occurs with <sup>2</sup>11 to form an

octahedral nickel(III) intermediate 212. In sharp contrast to the highly endergonic Ni(0)-Ni(II) oxidative addition, the Ni(III) intermediate <sup>2</sup>12 is only 6.3 kcal/mol more stable than <sup>2</sup>11. Complex 212 undergoes facile C-O reductive elimination via a five-membered cyclic TS (TS4). The Ni(III)-Ni(I) C-O RE requires a low barrier of 13.3 kcal/mol and is exergonic by 14.9 kcal/mol. The three-membered reductive elimination (TS4') is 10.4 kcal/mol less stable than TS4 (see Figure S5 for an even less favorable outer-sphere C-O RE involving a dissociated carbamate radical). Although the energy transfer-promoted C-O RE pathway via MLCT complex cannot be completely ruled out based on the computed barrier ( $\Delta G^{\ddagger}$  = 24.8 kcal/mol, vide supra), the Ni(I)-Ni(III) pathway was found to require lower barriers in both Ar-I oxidative addition and C-O RE steps. Therefore, the DFT calculations indicate that the Ni(I)-Ni(III) pathway is kinetically feasible once the catalytically active Ni(I) or Ni(III) species is generated.[21]

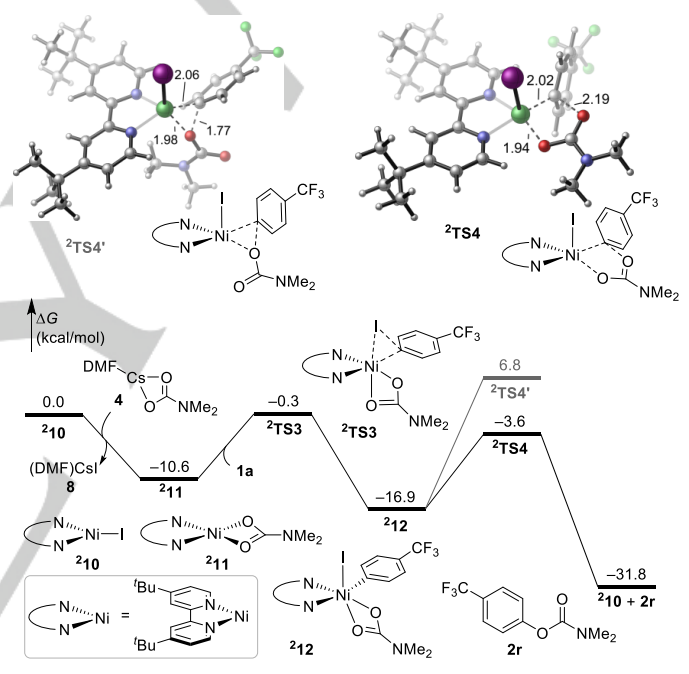


Figure 2. Computed reaction energy profile of the Ni(I)-Ni(III) pathway. 14

## Conclusion

We demonstrated that the carboxylative Buchwald-Hartwig amination could be performed under dual approach using an organophotocatalyst and an air stable Ni(II) precatalyst. The aryl carbamate derivatives have been synthesized under mild conditions of temperature and atmospheric pressure of CO2 tolerating a wide range of commercially available (hetero)aryl iodides and bromides, and amines. Moreover, preliminary mechanistic investigations including stoichiometric reactions as well as DFT calculations have been performed to discriminate between two plausible catalytic cycles: a Ni(0)-Ni(II) catalytic cycle under EnT catalysis and a Ni(I)-Ni(III) catalytic cycle through SET. Experimental data indicates the reduction of Ni(II) to generate an active Ni(I) catalyst as key step for the initiation of the catalytic cycle. Also, low barriers were required for both oxidative addition and C-O reductive elimination steps in the Ni(I)-Ni(III) cycle. Thus, these experimental and computational studies support a Ni(I)-Ni(III) pathway as a more likely route for the synthesis of aryl carbamate.

## **Experimental**

Synthesis of aryl carbamate: a 5 mL Snap vial was charged with aryl halide (0.2 mmol), NiBr2.diglyme (0.01 mmol, 5 mol%), dtbbpy (0.01 mmol), Cs2CO3 (0.4 mmol) and amine (0.4 mmol) successively. The vial was sealed and degassed under vacuum via syringe and filled with CO2 three times. Then, a solution of 5CzBn (0.1 mol% in 0.2 ml of DMF) and 1.8 mL of DMF were added to the vial. The vial was placed in between two 27 W bulb light (LED, 5-10 cm from either side of the vial), allowing temperature to rise to 40 °C due to the proximity of the lights. After 16 h, the solution was extracted three times with diethyl ether 30 mL. The combined organic phases were dried over Na<sub>2</sub>SO<sub>4</sub> and volatiles were evaporated. The crude product was further purified by flash column chromatography (SiO2, 10-20 % gradient of EtOAc in Pentane).

#### **Computational Details**

Density functional theory (DFT) and time-dependent DFT (TD-DFT) calculations were performed using Gaussian 16.30 All DFT geometry optimizations and vibrational frequency calculations were performed using the B3LYP-D3 functional31 with a mixed basis set of SDD32 for nickel, iodine, and cesium and 6-31G(d) for all other atoms in the gas phase. Single-point energy calculations were performed using the B3LYP-D3 functional with a mixed basis set of SDD for nickel, iodine, and cesium and 6-311+G(d,p) for all other atoms with solvation energy corrections. The solvation energy corrections were calculated in N,N-dimethylformamide (DMF) solvent with the SMD33 continuum solvation model. Because the excited metal-to-ligand charge transfer (MLCT) state leads to more polar structures, the geometries of triplet MLCT (tBubpy)Ni(aryl)(carbamate) complex 39(MLCT) and the C-O reductive elimination transition state 3TS2(MLCT) were optimized using TD-DFT in DMF solvent with the SMD solvation model. The TD-DFT geometry optimizations were performed at the firstexcited triplet state (see Figure S1 for molecular orbitals involved in this MLCT excited state) using the B3LYP functional with a mixed basis set of SDD for nickel and 6-31G(d) for all other atoms. Single point energies for TD-DFT calculations were also calculated with the B3LYP-D3 functional with a mixed basis set of SDD for nickel and 6-311+G(d,p) for all other atoms in DMF with the SMD solvation model. The triplet MLCT arylcarbamate product complex with Ni (316) is the triplet ground state. Therefore, this structure was optimized using DFT with the same functional and basis set as in the TD-DFT calculations [B3LYP-D3/SDD-6-311+G(d,p)/SMD(DMF)//B3LYP/SDD-6-31G(d)/SMD(DMF)]. The reported Gibbs free energies include thermal corrections calculated at 298.15 K.34-38

## **Acknowledgements**

This work was supported by the EMERGENCE@INC2022 action and the National Science Foundation (CHE-2247505). AT is deeply thankful to the INC-CNRS for their kind support. DFT

calculations were carried out at the University of Pittsburgh Center for Research Computing and the Advanced Cyberinfrastructure Coordination Ecosystem: Services & Support (ACCESS) program, supported by NSF award numbers OAC-2117681 and OAC-2138259. Y.Y and R. T thanks the the CSC (China Scholarship Council) for a doctoral fellowship. AT is thankful to Prof. Abderrahmane Amgoune and Dr. Julien. C. Vantourout (ICBMS Lyon) for fruitful discussions.

**Keywords:** Carboxylation • Buchwald-Hartwig • Dual catalysis • Density functional theory • Photochemistry

- a) Transition Metals for Organic Synthesis: Building Blocks and Fine Chemicals (Eds.: M. Beller, C. Bolm), 2nd ed., Wiley-VCH, Weinheim, 2004; b) Metal-Catalyzed Cross-Coupling Reactions (Eds.: A. de Meijere, F. Diedrich), 2nd ed., Wiley-VCH, Weinheim, 2004; c) P. Wolfe, S. Wagaw, J.-F. Marcoux, S. L. Buchwald, Acc. Chem. Res. 1998, 31, 805; d) J. F. Hartwig, Angew. Chem. 1998, 110, 2154; Angew. Chem. Int. Ed. 1998, 37, 2046; e) K. C. Nicolaou, P. G. Bulger, D. Sarlah, Angew. Chem. 2005, 117, 4516; Angew. Chem. Int. Ed. 2005, 44, 4442; f) G. Evano, N. Blanchard, M. Toumi, Chem. Rev. 2008, 108,3054; g) F. Monnier, M. Taillefer, Angew. Chem. 2009, 121, 7088; Angew. Chem. Int. Ed. 2009, 48, 6954; h) R. J. Lundgren, M. Stradiotto, Chem. Eur. J. 2012, 18,9758; i) P. Ruiz-Castillo, S. L. Buchwald, Chem. Rev. 2016, 116,12564; j) R. Dorel, C. P. Grugel, A. M. Haydl, Angew. Chem. 2019, 131, 17276; Angew. Chem. Int. Ed. 2019, 58, 17118.
- 2. C. Torborg, M. Beller, Adv. Synth. Catal. 2009, 351, 3027.
- a) X.-F. Wu, H. Neumann, M. Beller, Chem. Soc. Rev. 2011, 40, 4986;
   b) A. Brennführer, H. Neumann, M. Beller, Angew. Chem. 2009, 121, 4176; Angew. Chem. Int. Ed. 2009, 48, 4114;
   c) X.-F. Wu, H. Neumann, M. Beller, Chem. Rev. 2013, 113, 1.
- a) C. F. Bernard, Organometallics 2008, 27, 5402; for selected examples see: b) J. R. Martinelli, T. P. Clark, D. A. Watson, R. H. Munday, S. L. Buchwald, Angew. Chem. 2007, 119, 8612; Angew. Chem. Int. Ed. 2007, 46, 8460; c) X.-F. Wu, H. Neumann, M. Beller, Chem. Eur. J. 2010, 16, 9750; d) P. Hermange, A. T. Lindhardt, R. H. Taaning, K. Bjerglund, D. Lupp, T. Skrydstrup, J. Am. Chem. Soc. 2011, 133, 6061; d) P. G. Alsabeh, M. Stradiotto, H. Neumann, M. Beller, Adv. Synth. Catal. 2012, 354, 3065.
- K. W. Quasdorf, A. Antoft-Finch, P. Liu, A. L. Silberstein, A. Komaromi, T. Blackburn, S. D. Ramgren, K. N. Houk, V. Snieckus, N. K. Garg, J. Am. Chem. Soc. 2011. 133. 6352-6363.
- a) S. Topham in Ullmann's Encyclopedia, Wiley-VCH, Weinheim, 2001;b)
   G. Centi, E.A. Quadrelli, S. Perathoner, Energy Environ. Sci. 2013, 6, 1711; c) M. Aresta, A. Dibenedetto, A. Angelini, Chem. Rev. 2014, 114, 1709. d) J. Klankermayer, S. Wesselbaum, K. Beydoun, W. Leitner, Angew. Chem. 2016, 128,7416; Angew. Chem. Int. Ed. 2016, 55, 7296; e) Y. Li, X. Cui, K. Dong, K. Junge, M. Beller, ACS Catal. 2017, 7,1077; f) J. Artz, T. E. Müller, K. Thenert, J. Kleinekorte, R. Meys, A. Sternberg, A. Bardow, W. Leitner, Chem. Rev. 2018, 118, 434; j) J. Klankermayer, S. Wesselbaum, K. Beydoun, W. Leitner, Angew. Chem. 2016, 128, 7416; Angew. Chem. Int. Ed. 2016, 55,7296; k) R. Cauwenbergh, V. Goyal, R. Maiti, K. Natte, S. Das, Chem. Soc. Rev. 2022, 22, 9371.
- a) A. K. Ghosh, M. Brindisi, J. Med. Chem. 2015, 58, 2895; b) R. B. Watson, T. W. Butler, J. C. DeForest, Org. Process Res, Dev. 2021, 25, 500; for exempels using CO<sub>2</sub> please see: the use of diaryliodonium slats c) W. Xiong, C. Qi, Y. Peng, T. Guo, M. Zhang, H. Jiang, Chem. Eur. J. 2015, 21, 14314; starting with aryl boronic acids derivatives see: d) W. Xiong, C. Qi, T. Guo, M. Zhang, K. Chen, H. Jiang, Green Chem. 2017, 19, 1642; d) With sulfonium salts: Y. Guo, L. Wei, Z. Wen, H. Jiang, C. Qi, Chem. Commun. 2023, 59, 764.
- a) W. Schilling, S. Das, ChemSusChem 2020, 13, 6246; b) V. Aomchad,
   À. Cristòfol, F. Della Monica, B. Limburg, V. D'Elia, A.W. Kleij, Green Chem. 2021, 23, 1077; from the transformation of carbamate addcuts from our laboratory please see: c) K. Onida, A. Tlili, Angew. Chem. 2019, 131, 12675; Angew. Chem. Int. Ed. 2019, 58, 12545; d) A. Taponard, T.

- Jarrosson, L. Khrouz, M. Médebielle, J. Broggi, A. Tilli, *Angew. Chem.* **2022**, *134*, e202204623; *Angew. Chem. Int. Ed.* **2022**, *61*, e202204623;
- a) E. R. Welin, C. Le, D. M. Arias-Rotondo, J. K. McCusker, D. W. C. MacMillan, *Science* 2017, 355, 380; b) L. Tian, N. A. Till, B. Kudisch, D. W. C. Macmillan, G. D. Scholes, *J. Am. Chem. Soc.* 2020, 142, 4555.
- J. Lu, B. Pattengale, Q. Liu, S. Yang, W. Shi, S. Li, J. Huang, J. Zhang, J. Am. Chem. Soc. 2018, 140, 13719.
- For selected reviews on dual photoredox/nickel catalysis see: a) J. Twilton, C. Le, P. Zhang, M. H. Shaw, R. W. Evans, D. W. C. Nat. Chem. Rev. 2017, 1, 52; b) J. A. Milligan, J. P. Phelan, S. O. Badir, G. A. Molander, Angew. Chem. 2019, 131, 6212; Angew. Chem. Int. Ed. 2019, 58, 6152; c) C. Zhu, H. Yue, L. Chu, M. Rueping, Chem. Sci., 2020, 11, 4051.
- While preparing this manuscript a related study appeared please see: A.
   Sahari, J. Puumi, J. K. Mannisto, T. Repo, J. Org. Chem. 2023, 88, 3822.
- B. J. Shields, B. Kudisch, G. D. Scholes, A. G. Doyle, J. Am. Chem. Soc. 2018, 140, 3035.
- a) D. A. Cagan, D. Bím, D. B. Silva, N. P. Kazmierczak, B. J. McNicholas,
   R. G. Hadt, J. Am. Chem. Soc. 2022, 144, 6516; b) D. A. Cagan, G. D.
   Stroscio, A. Q. Cusumano, R. G. Hadt, J. Phys. Chem. A 2020, 124, 9915.
- 14. DFT calculations were performed at the B3LYP-D3/SDD-6-311+G(d,p)/SMD(DMF)//B3LYP-D3/SDD-6-31G(d) level of theory. TD-DFT calculations were performed at the B3LYP-D3/SDD-6-311+G(d,p)/SMD(DMF)//B3LYP/SDD-6-31G(d)/SMD(DMF) level of theory. See SI for computational details.
- For a computational study on the mechanism of carbamate formation, see: R. B. Said, J. M. Kolle, K. Essalah, B. Tangour, A. Sayari, ACS Omega, 2020, 5, 26125-26133.
- a) P. Ma, S. Wang, H. Chen, ACS Catal., 2020, 10, 1-6. b) Y. Dong, Z.
   Zhao, Y. Geng, Z. Su, B. Zhu, W. Guan, Inorg. Chem., 2023, 62, 1156.
- K. W. Quasdorf, A. Antoft-Finch, P. Liu, A. L. Silberstein, A. Komaromi, T. Blackburn, S. D. Ramgren, K. N. Houk, V. Snieckus, N. K. Garg, J. Am. Chem. Soc. 2011, 133, 6352.
- Alternatively, Ni(II) species may be excited to a triplet d-d state. However, previous computational studies suggested that the excitation-promoted C-O RE involves the MLCT state, rather than the d-d excited state. See: 16a.
- Our DFT claculations indiciated this SET process is exergonic by 25.1 kcal/mol. See SI for details. For a previous computational study of a similar process, see ref. 16b.
- B. Maity, T. R. Scott, G. D. Stroscio, L. Gagliardi, L. Cavallo, ACS Catal. 2022, 12, 13215.
- 21. Under the optimum conditions starting with NiB<sub>2</sub>.digliyme, subjecting 4-MeOPhI as aryl halide coupling partner, only traces of the desired product were obtained. However, by using Ni(cod)<sub>2</sub> as precatalyst allows the formation of the desired coupling product in 30% yield. Thus, we assume that different reaction pathway could take place depending on the nature of the starting Ni precatalyst.
- W. Xiong, C. Qi, T. Guo, M., Zhang, K. Chen, H. Jiang, Green Chem., 2017. 19. 1642.
- W. Xiong, C. Qi, Y. Peng, T. Guo, M. Zhang, , H. Jiang, *Chem. Eur. J.*, 2015, 21, 14314.
- P. Leowanawat, N. Zhang, V. Percec, J. Org. Chem., 2012, 77, 1018– 1025.
- 25. S. E. Varjosaari, P. Suating, M. J. Adler, Synthesis, 2016, 48, 43.
- K. W. Quasdorf, M. Riener, K. V. Petrova and N. K. Garg, *J. Am. Chem. Soc.*, 2009, 131, 17748.
- 27. Y. G. Zhao, V. Snieckus, J. Am. Chem. Soc., 2014, 136, 11224.
- S. A. Swanger, K. M. Vance, T. M. Acker, S. S. Zimmerman, J. O. Di Raddo, S. J. Myers, C. Bundgaard, C. A. Mosley, S. L. Summer, D. S. Menaldino, H. S. Jensen, D. C. Liotta, S. F. Traynelis, ACS Chem. Neurosci., 2018, 9, 306.
- 29. L. Guo, H. -Y. Tu, S. Zhu, L. Chu, Org. Lett. 2019, 21, 4771.
- Gaussian 16, Revision C.01, M. J. Frisch, G. W. Trucks, H. B. Schlegel, G. E. Scuseria, M. A. Robb, J. R. Cheeseman, G. Scalmani, V. Barone, G. A. Petersson, H. Nakatsuji, X. Li, M. Caricato, A. V. Marenich, J. Bloino, B. G. Janesko, R. Gomperts, B. Mennucci, H. P. Hratchian, J. V. Ortiz, A. F. Izmaylov, J. L. Sonnenberg, D. Williams-Young, F. Ding, F. Lipparini, F. Egidi, J. Goings, B. Peng, A. Petrone, T. Henderson, D.

- Ranasinghe, V. G. Zakrzewski, J. Gao, N. Rega, G. Zheng, W. Liang, M. Hada, M. Ehara, K. Toyota, R. Fukuda, J. Hasegawa, M. Ishida, T. Nakajima, Y. Honda, O. Kitao, H. Nakai, T. Vreven, K. Throssell, J. A. Montgomery, Jr., J. E. Peralta, F. Ogliaro, M. J. Bearpark, J. J. Heyd, E. N. Brothers, K. N. Kudin, V. N. Staroverov, T. A. Keith, R. Kobayashi, J. Normand, K. Raghavachari, A. P. Rendell, J. C. Burant, S. S. Iyengar, J. Tomasi, M. Cossi, J. M. Millam, M. Klene, C. Adamo, R. Cammi, J. W. Ochterski, R. L. Martin, K. Morokuma, O. Farkas, J. B. Foresman, and D. J. Fox, Gaussian, Inc., Wallingford CT, 2016.
- (a) C. Lee, W. Yang, R. G. Parr, *Phys. Rev. B.* 1988, 37, 785. (b) A. D. Becke, *J. Chem. Phys.* 1993, 98, 5648. (c) S. Grimme, J. Antony, S. Ehrlich, H. Krieg, *J. Chem. Phys.*, 2010, 132, 154104.
- D. Andrae, U. Haeussermann, M. Dolg, H. Stoll, H. Preuss, *Theor. Chem. Acc.* 1990, 77, 123.
- A. V. Marenich, C. J. Cramer, D. G. Truhlar, J. Phys. Chem. B, 2009, 113, 6378.
- a) B. J. Shields, B. Kudisch, G. D. Scholes, A. G. Doyle, *J. Am. Chem. Soc.* 2018, 140, 3035; b) D. A. Cagan, D. Bím, D. B. Silva, N. P. Kazmierczak, B. J. McNicholas, R. G. Hadt, *J. Am. Chem. Soc.* 2022, 144, 6516; c) D. A. Cagan, G. D. Stroscio, A. Q. Cusumano, R. G. Hadt, *J. Phys. Chem. A* 2020, 124, 9915.
- Y. Dong, Z. Zhao, Y. Geng, Z. Su, B. Zhu, W. Guan, *Inorg. Chem.*, 2023, 62, 1156.
- a) J. E. Bartmess, J. Phys. Chem. 1994, 98, 6420; b) J. E. Bartmess, J. Phys. Chem. 1995, 99, 6755.
- (a) E. Speckmeier, T. G. Fischer, K. Zeitler, J. Am. Chem. Soc. 2018, 140, 15353-15365. (b) M. A. Bryden, E. Zysman-Colman, Chem. Soc. Rev., 2021, 50, 7587–7680.
- 38. A. A. Isse, A. Gennaro, J. Phys. Chem. B 2010, 114, 7894-7899.

# **Entry for the Table of Contents**

Air stable Ni - Organophotocatalyst - Mechanism - DFT

The carboxylative Buchwald-Hartwig amination is disclosed herein under mild conditions of temperature and under atmospheric pressure of CO<sub>2</sub>. The key to success is the use of a dual strategy organophotocatalysis/nickel catalysis under visible light irradiation. The developed conditions demonstrated high functional group tolerance toward (hetero)aryl iodide and bromide. Furthermore, preliminary mechanistic investigations including stoichiometric reactions and DFT calculations shed light on the reaction mechanism.

Institute and/or researcher Twitter usernames: ((optional))